Research Article

Journal of MASS SPECTROMETRY

Received: 28 October 2011 Revised: 25 February 2011 Accepted: 5 March 2011 Published online in Wiley Online Library

(wileyonlinelibrary.com) DOI 10.1002/jms.2986

Fragmentation of oxime and silyl oxime ether odd-electron positive ions by the McLafferty rearrangement: new insights on structural factors that promote α,β fragmentation

Sébastien Laulhé,[a] Bogdan Bogdanov,[b]* Leah M. Johannes,[a] Osvaldo Gutierrez,[c] Jason G. Harrison,[c] Dean J. Tantillo,[c] Xiang Zhang[a] and Michael H. Nantz[a]*

The McLafferty rearrangement is an extensively studied fragmentation reaction for the odd-electron positive ions from a diverse range of functional groups and molecules. Here, we present experimental and theoretical results of 12 model compounds that were synthesized and investigated by GC-TOF MS and density functional theory calculations. These compounds consisted of three main groups: carbonyls, oximes and silyl oxime ethers. In all electron ionization mass spectra, the fragment ions that could be attributed to the occurrence of a McLafferty rearrangement were observed. For *t*-butyldimethylsilyl oxime ethers with oxygen in a β-position, the McLafferty rearrangement was accompanied by loss of the *t*-butyl radical. The various mass spectra showed that the McLafferty rearrangement is relatively enhanced compared with other primary fragmentation reactions by the following factors: oxime *versus* carbonyl, oxygen *versus* methylene at the β-position and ketone *versus* aldehyde. Calculations predict that the stepwise mechanism is favored over the concerted mechanism for all but one compound. For carbonyl compounds, C–C bond breaking was the rate-determining step. However, for both the oximes and *t*-butyldimethylsilyl oxime ethers with oxygen at the β-position, the hydrogen transfer step was rate limiting, whereas with a CH_2 group at the β-position, the C–C bond breaking was again rate determining. *n*-Propoxy-acetaldehyde, bearing an oxygen atom at the β-position, is the only case that was predicted to proceed through a concerted mechanism. The synthesized oximes exist as both the (*E*)- and (*Z*)-isomers, and these were separable by GC. In the mass spectra of the two isomers, fragment ions that were generated by the McLafferty rearrangement were observed. Finally, fragment ions corresponding to the McLafferty reverse charge rearrangement were observed for all compounds at varying relative ion intensities compared with the conventional McLafferty rearrangement. Copyright © 2012 John Wiley & Sons, Ltd.

Supporting information may be found in the online version of this article.

Keywords: silyl oxime ethers; GC-TOF MS; concerted; stepwise; computational study

INTRODUCTION

The analysis of cellular aldehyde and ketone species is of considerable importance for the field of metabolomics. [1–3] Aldehydes and ketones can be formed endogenously by various biochemical pathways. For example, aldehydes can be formed by lipid peroxidation, carbohydrate metabolism and ascorbate autoxidation as well as by various enzymatic processes, such as those involving amine oxidase, cytochrome P-450 or myeloperoxidase. [4] Endogenous ketones, such as acetone and acetoacetic acid, are molecules produced as by-products when fatty acids are broken down for energy in the liver and kidney. [5] Other ketones, such as β-ketopentanoate, may be created as a result of the metabolism of synthetic triglycerides. [6] Furthermore, ketone bodies, such as acetone, are produced from acetyl-CoA mainly in the mitochondrial matrix of hepatocytes when carbohydrates are so scarce that energy must be obtained from breaking down fatty acids. [7] Acetone is responsible for the characteristic "fruity" odor of the breath of persons with ketoacidosis. [8]

To isolate these carbonyl metabolites for analysis by mass spectrometry, their selective conversion into labeled oximes or oxime ether analogs by water-based "click chemistry" (i.e. oximation) has become an elegant and highly chemo-specific approach. [9,10] Oxime chemistry and subsequent silylations to form silyl oxime ethers have been used to detect and analyze natural and synthetic steroids, [11] trisaccharides [12–15] and other classes of compounds [16,17] by gas chromatography–mass spectrometry (GC-MS). Oximation proceeds rapidly under

* *Correspondence to: Bogdan Bogdanov, Department of Chemistry, University of the Pacific, Stockton, California 95211, USA. E-mail: bbogdano@pacific.edu Michael H. Nantz, Department of Chemistry, University of Louisville, Louisville, Kentucky 40292, USA. E-mail: michael.nantz@louisville.edu*

a *University of Louisville, Department of Chemistry, Louisville, Kentucky 40292, USA*

b *University of the Pacific, Department of Chemistry, Stockton, California 95211, USA*

c *University of California, Department of Chemistry, Davis, California 95616, USA*

Copyright © 2012 John Wiley & Sons, Ltd.

Journal of MASS SPECTROMETRY

mild conditions and is chemoselective in that the aminooxy reaction with carbonyl groups is preferred over the majority of other functionalities. Among other advantages, oxime ethers are potentially suitable as components of dynamic libraries. [18] The study of the major MS fragmentations of these carbonyl derivatives, however, has not received due attention. For example, although the McLafferty rearrangement [19,20] of carbonyl compounds has been the focus of extensive and continuous research [21–60], studies on oximes and silyl oxime ethers have been limited. [9–17,37] Surprisingly, to date, only one article has reported the McLafferty rearrangement for ketoximes. Bowen and Maccoll observed both single and double McLafferty rearrangement fragments in the mass spectra of various ketoximes under low-energy (12 eV) and low-temperature (350 K) ionization. [37]

The characteristics of the McLafferty rearrangement have been described extensively and in great detail. [29] Briefly, the McLafferty rearrangement involves the transfer of an aliphatic hydrogen atom from a γ-position to an acceptor group. Carbonyl groups in ketones, aldehydes, carboxylic acids, esters, amides and other derivatives are the most common acceptor groups, but aromatic and heteroaromatic rings can also act as acceptors. Not only does the γ-hydrogen atom have to be bound to an sp^3-hybridized carbon atom, it also has to be sterically accessible to the acceptor group. Hydrogen atom transfer is accompanied by the cleavage of the α–β bond, and this results in the formation of an odd-electron positive ion (enol ion) and a neutral molecule (Scheme 1).

In addition, the McLafferty rearrangement is known to occur with a reverse charge distribution, i.e. generating the neutral enol and the charged alkene fragments. [61]

The McLafferty rearrangement can proceed through either a concerted or stepwise mechanism. [29] Various elegant experiments have been performed to probe the mechanistic nature of the McLafferty rearrangement, and to date, in all cases, the results point toward the stepwise mechanism. [33,39,42,53,57] Various theoretical studies have been performed that confirmed the stepwise mechanism, but some also identified systems that should or could proceed through the concerted mechanism. [23,38,40,48,65] Finally, in addition to the single hydrogen transfer McLafferty rearrangement, consecutive rearrangements that proceed by a double hydrogen transfer have been reported. [29] In general, one would expect that the McLafferty rearrangement will have to compete with other fragmentation pathways, such as simple bond cleavages that are entropically more favorable. [29] The relative importance of the various fragmentation pathways is determined by their respective kinetics inside the ion source, which is related to the thermochemistry, and can be calculated fairly accurately by applying the Rice-Ramsperger-Kassel-Marcus (RRKM) theory. [62–64] In most cases, the potential energy surfaces of the different fragmentation pathways need to be known, and quantum chemical calculations can provide the input parameters for the RRKM calculations. [65]

In this article, we report the GC-TOF MS mass spectra for a panel of carbonyl, oxime and silyl oxime ether substrates. We also disclose a systematic computational investigation into the McLafferty rearrangements observed for most of the compound panel to obtain more insight into the intrinsic factors that promote and determine the nature of the McLafferty rearrangement. In particular, we examine the influence of oxygen substitution adjacent to the site of hydrogen atom abstraction in the McLafferty rearrangement as a potential means to promote the fragmentation.

EXPERIMENTAL SECTION

Synthesis and structural characterization

The 12-model compounds used in this study (Fig. 1) were either purchased or synthesized as described in the accompanying Supporting Information.

Gas chromatography–mass spectrometry

The GC/TOF-MS analyses were performed on a LECO Pegasus® 4D time-of-flight mass spectrometer (LECO Corporation, St. Joseph, MI) equipped with a Gerstel MPS2 auto-sampler (GERSTEL Inc, Linthicum, MD). The Pegasus 4D GC × GC/TOF-MS instrument was equipped with an Agilent 6890 gas chromatograph featuring a LECO two-stage cryogenic modulator and a secondary oven. A 30 m × 0.25 mm ^1d_c × 0.25 μm ^1d_f, DB-225 GC capillary column [(50%-phenyl)-dimethylpolysiloxane] (Agilent Technologies J&W, Santa Clara, CA) was used as the primary column for the GC × GC/TOF-MS analysis. A second column of

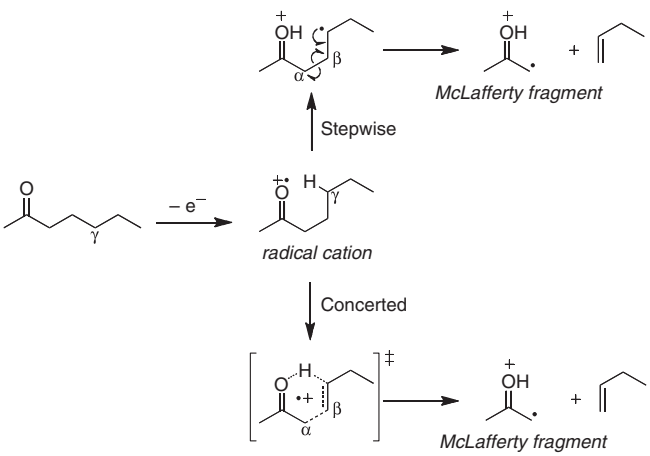

Scheme 1. The stepwise and concerted McLafferty rearrangement mechanisms.

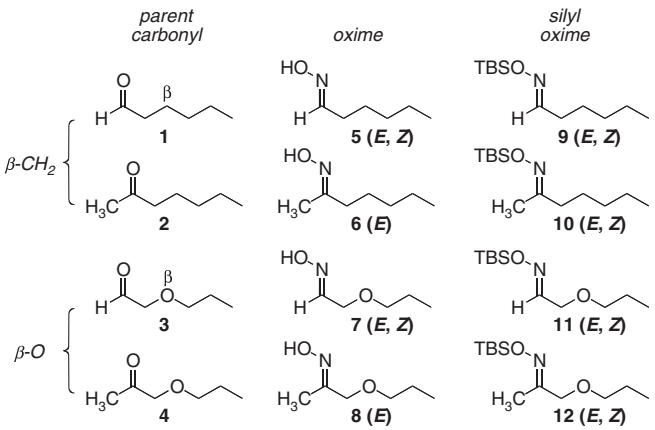

Figure 1. Aldehyde and ketone panel. TBS = $SiMe_2t$-Bu.

 Copyright © 2012 John Wiley & Sons, Ltd.

2 m × 0.18 mm ^2d_c × 0.25 μm ^2d_f, DB-5MS [(5%-cyanopropylphenyl)-dimethylpolysiloxane] (Agilent Technologies J&W, Santa Clara, CA) was placed inside the secondary oven after the thermal modulator. The helium carrier gas flow rate was set to 1.0 ml/min at a corrected constant flow via pressure ramps. A 2.0 μl liquid sample was injected into the liner using the split mode (25 : 1), with the injection port temperature set at 250 °C. The primary column temperature was programmed with an initial temperature of 60 °C for 0.5 min and then increased at a rate of 10 °C/min to 210 °C. The secondary column temperature program was set to an initial temperature of 65 °C for 0.5 min and then increased at the same temperature gradient employed in the first column up to a temperature of 215 °C accordingly. The thermal modulator was set to +20 °C relative to the primary oven, and a modulation time of 0 s was used, which allowed the instrument to be operated in the GC/TOF-MS mode. The MS mass range was m/z = 25–500 with an acquisition rate of 10 spectra per second. The ion source chamber was set at 230 °C with the MS transfer line temperature set to 225 °C, the detector voltage was set at 1600 V, and the electron energy for ionization was set at 70 eV. The ion acceleration voltage was turned on after a solvent delay of 168 s. LECO's ChromaTOF software package (version 4.21) equipped with the National Institute of Standards and Technology (NIST) MS database (NIST MS Search 2.0, NIST/EPA/NIH Mass Spectral Library; NIST 2002) was used for instrument control, spectrum deconvolution and metabolite identification in all experiments. These parameters are baseline offset = 0.5; smoothing = auto; peak width = 1 s; signal-to-noise ratio (S/N) = 4; mass threshold = 100; minimum forward similarity match before name is assigned = 600. The peak true spectrum was also exported as part of the information for each peak in absolute format of intensity values.

Quantum chemical calculations

All structures were optimized at the UB3LYP/6-31 G(d) level of theory [66] with the guess = (mix,always) keyword as implemented in the *GAUSSIAN03* suite of programs [67], unless otherwise noted. Some selected structures were also optimized at the UB3LYP/6-311++G(2 d,2p) level of theory to investigate the effect of a larger basis set. Although B3LYP has been used previously, with success, for studies of neutral and radical cation pericyclic reactions, [68] selected structures were also optimized using UM06-2X/6-31 G(d), [69] UMP2/6-31 G(d) [70] and SCS-UMP2/6-31 G(d) [71] as implemented in *GAUSSIAN09* [72] see Supporting Information for details). All stationary points were characterized as minima or transition state structures by vibrational analysis, and intrinsic reaction coordinate calculations [73] were performed for selected transition state structures to confirm their connections to surrounding minima. Structural drawings were produced using Ball & Stick. [74]

RESULTS AND DISCUSSION

In the Supporting Information, the 70 eV electron ionization mass spectra of the 12 synthesized model compounds are shown, as well as the NMR spectra of new compounds. In all, the fragment ions resulting from the McLafferty rearrangement are present to varying extents. Our GC-TOF MS spectra showed high similarities with the previously published mass spectra of compounds **1** and **2**. [75,76] In all mass spectra, except of compound **2**, no molecular ions ($M^{+\bullet}$) can be observed. As expected, numerous fragment ions have been generated from the excited molecular ions ($M^{+\bullet *}$) that were generated due to electron ionization in the ion source, especially the ones resulting from simple and favorable bond cleavages. Due to the presence of numerous fragment ions, it is challenging to determine the normalized intensity of McLafferty rearrangement fragment ions and to perform some kind of semiquantification to compare the various entries. By comparing compounds **1** and **2**, it is clear that ketone functionality enhances the McLafferty rearrangement compared with the aldehyde functionality. A similar pattern is observed when comparing compounds **3** and **4**, and this pattern is in agreement with the relative basicity of the carbonyl oxygens. However, in contrast to expectations, when comparing compounds **1** and **3**, it seems that introduction of oxygen on the β-position suppresses the McLafferty rearrangement, and a similar observation can be made when comparing compounds **2** and **4**, although the extent is much less. In the case of ketone **4**, the β-oxygen appears to significantly promote fragmentation via carbonyl alpha cleavage to generate the corresponding acylium ion $H_3CC{\equiv}O^+$ (m/z = 43) by stabilization of the leaving radical fragment $^{\bullet}CH_2On$-Pr.

The synthesis of the oximes (**5–8**) and silyl oxime ethers (**9–12**) gave rise to both the (*E*)- and (*Z*)-isomers (except for ketoximes **6** and **8** that were formed in lower *E*/*Z* ratios). In the ^{1}H NMR spectra of these two isomers, unique peaks could be observed, and these were used to determine the *E*/*Z* ratio. Data are summarized in Table 1.

In the total ion chromatograms of the GC-TOF MS experiments, two peaks could be observed (except for **6** and **8** where only the (*E*)-isomers were detected), originating from the (*E*)- and (*Z*)-isomers. There was only partial agreement between the E/Z ratios determined by ^{1}H NMR and by GC-MS. It could be concluded that extensive (*Z*)-to-(*E*) isomerization might have taken place in the GC column or in the heated transfer line. In the case of the isolated oxime fragment (aldehyde system), the (*Z*)-isomer is 0.1 kcal/mol lower in energy than the (*E*)-isomer. The barrier height for (*E*)-to-(*Z*) isomerization is predicted to be 16.2 kcal/mol in the ionized state, although it is predicted to be 18.5 kcal/mol for the ketone system [UB3LYP/6-31G(d)]. These results do not confirm or exclude isomerization in the ion source as an alternative. In the case of compounds **5–8**, the McLafferty rearrangement is more pronounced in the mass spectra of the (*E*)-isomers than of the (*Z*)-isomers. No direct McLafferty rearrangement fragment ions can be observed in the mass spectra of the silyl oxime ethers **9–12**. However, fragment ions derived from loss of *t*-butyl radical after McLafferty rearrangement are observed in the mass spectra of compounds **11** and **12** (Table 2).

Loss of the *t*-butyl radical followed by McLafferty rearrangement does not seem plausible for the first loss would create an even electron ion. Although the McLafferty rearrangement has been observed for even electron systems [21,22,24,25,30–32,36,41,46,49,60], it seems unlikely to be of great importance for these systems, but it cannot be excluded for we did not investigate this possibility in more detail. The loss of just the *t*-butyl radical was also observed as the peaks at the highest m/z values, as well as abundant formation of $[HOSi(CH_3)_2]^+$

Copyright © 2012 John Wiley & Sons, Ltd.

Journal of MASS SPECTROMETRY

Table 1. Overview of the observed ^{1}H NMR *E/Z* ratios for entries **5–12**

Class	Compound	^{1}H NMR[a] *E/Z* ratio	^{1}H NMR shift[b] (ppm)	GC–MS retention time *E, Z* (s)
Oxime	**5**	1 : 0.7	$-H_E$: δ 7.42	468, 486
	Aldoxime		$-H_Z$: δ 6.72	
	6	1 : 0.3	$(-CH_2-)_E$: δ 2.17	506 (*E*)-isomer only
	Ketoxime		$(-CH_2-)_Z$: δ 2.36	
	7	1 : 0.8	$-H_E$: δ 7.50	510, 515
	Aldoxime		$-H_Z$: δ 6.92	
	8	1 : 0.17	$(-CH_2O-)_E$: δ 3.98	527 (*E*)-isomer only
	Ketoxime		$(-CH_2O-)_Z$: δ 4.32	
Silyl–oxime ether	**9**	1 : 1	$-H_E$: δ 7.49	488, 479
	Aldoxime		$-H_Z$: δ 6.85	
	10	1 : 0.3	$(-CH_2-)_E$: δ 2.17	490, 473
	Ketoxime		$(-CH_2-)_Z$: δ 2.34	
	11	1 : 1	$-H_E$: δ 7.56	512, 501
	Aldoxime		$-H_Z$: δ 7.03	
	12	1 : 0.2	$(-CH_2O-)_E$: δ 3.99	500, 494
	Ketoxime		$(-CH_2O-)_Z$: δ 4.31	

[a]400 MHz, taken in $CDCl_3$.
[b]Values given for oximyl-H (**5**, **7**, **9**, **11**), C(3) methylene (**6**, **10**) or C(3) methylene (**8**, **12**).

Table 2. Overview of the observed McLafferty rearrangement features in the 70 eV EI mass spectra

				McLafferty rearrangement fragment		McLafferty reverse charge rearrangement fragment	
Compound	Elemental composition	$M^{+\bullet}$ *m/z*	$M^{+\bullet}$ ion count	*m/z*	ion count[a]	*m/z*	ion count[a]
1	$C_6H_{12}O$	100	Not observed	44	1000	56	585
2	$C_7H_{14}O$	114	< 50	58	420	56	15
3	$C_5H_{10}O_2$	102	Not observed	44	88	58	20
4	$C_6H_{12}O_2$	116	Not observed	58	180	58	180 (same *m/z* as McLafferty)
5	$C_6H_{13}ON$	115	Not observed	59	(*E*), 1000; (*Z*), 660	56	(*E*), 305; (*Z*), 270
6	$C_7H_{15}ON$	129	Not observed	73	(*E*), 1000	56	(*E*), 80
7	$C_5H_{11}O_2N$	117	Not observed	59	(*E*), 1000; (*Z*), 390	58	(*E*), 700; (*Z*), 98
8	$C_6H_{13}O_2N$	131	Not observed	73	(*E*), 1000	58	(*E*), 120
9	$C_{12}H_{27}ONSi$	229	Not observed	173	(*E*), not observed; (*Z*), not observed	56	(*E*), 40; (*Z*), 30
				116 [b]	(*E*), < 5; (*Z*), < 5		
10	$C_{13}H_{29}ONSi$	243	Not observed	187	(*E*), not observed; (*Z*), not observed	56	(*E*), 75; (*Z*), 70
				130 [b]	(*E*), < 10; (*Z*), < 5		
11	$C_{11}H_{25}O_2NSi$	231	Not observed	173	(*E*), not observed; (*Z*), not observed	58	(*E*), 70; (*Z*), 65
				116 [b]	(*E*), 188; (*Z*), 85		
12	$C_{12}H_{27}O_2NSi$	245	Not observed	187	(*E*), not observed; (*Z*), not observed	58	(*E*), 68; (*Z*), 60
				130 [b]	(*E*), 170; (*Z*), 106		

[a]Major fragment ion assigned a relative value of 1000.
[b]McLafferty rearrangement fragment minus *t*-Bu$^\bullet$.

(*m/z* = 75). These reactions will be discussed in more detail in the next sections.

In addition to the conventional McLafferty rearrangement reaction, the fragment ions corresponding to the McLafferty reverse charge rearrangement [61] were observed. For compound **4**, the fragment ions of both reactions have the same *m/z* values and cannot be distinguished, and neither can their relative contributions be estimated. The occurrence of the McLafferty reverse charge rearrangement is an indication that the McLafferty rearrangement actually took place, and so the relative contributions should be added to obtain a quantitative estimate of the overall contribution of the McLafferty rearrangement reaction. For entries **1**, **3**, **5**, **7** and **9–12**, the McLafferty reverse charge rearrangement had contributions of >25% relative to the McLafferty rearrangement. For entries **5** and **7**, the relative contributions were different for the (*E*)- and (*Z*)-isomers. Data in the Supporting Information show that the oxygen atom at the β-position (Y=O, Scheme 2) and the aldehyde functionality (R=H) strongly favor the McLafferty reverse charge rearrangement energetically compared with

 Copyright © 2012 John Wiley & Sons, Ltd.

Y=CH_2 and R=CH_3. The identity of the acceptor group (X=O, NOH and $NOSiH_3$) was of less importance. Surprisingly, the relative stabilities of the ionic and neutral products of the two reactions do not always determine which process is more favorable (Supporting Information) nor can it explain the sometimes close competitiveness. For entries **1**, **3** and **8**, the McLafferty reverse charge rearrangement is energetically more favorable, whereas the McLafferty rearrangement is more abundant like for all other entries except **9** and **10**. However, it was beyond the scope of this article to theoretically investigate the McLafferty reverse charge rearrangement in more detail, which would be needed to provide a more quantitative discussion and comparison.

As shown in Scheme 2, fragmentation can proceed through a concerted McLafferty rearrangement (**A**$^{\bullet+}$→**G**$^{\bullet+\ddagger}$→**E**$^{\bullet+}$+**F**) or via a stepwise hydrogen transfer/cleavage process (red; **A**$^{\bullet+}$→**B**$^{\bullet+\ddagger}$→**C**$^{\bullet+}$→**D**$^{\bullet+\ddagger}$→**E**$^{\bullet+}$+**F**). Our calculations indicate that for all systems, with the exception of ethoxyethanal (R=H, X=Y=O; Table 3, compound 3), the stepwise pathway is favored. [77] Barriers for both steps are somewhat sensitive to the identity of X and Y (Table 3). Among the three classes of compounds studied, aldehydes/ketones are predicted to have the largest overall energy barriers, whereas oximes have the lowest. Introduction of a more electronegative group at the β-position is expected to facilitate the cleavage of the α–β bond, and this is the case for all systems examined herein (Y=CH_2 *vs* Y=O). Consequently, for the oximes and silyl oxime ethers with Y=O, the rate-determining step is predicted to be the initial hydrogen transfer step. Although changing from Y=CH_2 to Y=O might be expected to help the hydrogen transfer step as well, because an oxygen can interact favorably with an attached carbon radical, we do not see evidence for this effect. Although fragmentation reactions take place from initially excited molecular ions, an extensive treatment of excitation processes is beyond the scope of this article. Nonetheless, our results reveal the underlying potential energy surfaces for the fragmentation reactions. For entries **9–12**, calculations were also performed using the larger 6-311++G (2d,2p) basis set; qualitatively similar results were observed (Table 3).

Representative computed transition state structures are shown in Fig. 2. For the one system where a concerted process was predicted to be energetically preferred (X=Y=O), this process was found to involve asynchronous hydrogen transfer and cleavage events. In the transition state structure for this process (**3 G**$^{\bullet+\ddagger}$ in Fig. 2), hydrogen transfer is nearly complete, whereas the C–O bond cleavage has not yet begun. As mentioned earlier, changing the identity of X and/or Y leads to a stepwise mechanism where hydrogen transfer occurs first. A representative transition state structure for hydrogen transfer (**5B**$^{\bullet+\ddagger}$) is also shown in Fig. 2. In contrast to **3 G**$^{\bullet+\ddagger}$, this transition state structure is early with respect to the hydrogen transfer event; the migrating hydrogen is closer to the carbon from which it originates than to its destination on nitrogen (note that an even earlier transition state structure is predicted with UM06-2X). Changing from Y=CH_2 to Y=O (**7B**$^{\bullet+\ddagger}$) leads to a later transition state structure, however, in which the C–H and H–N distances are similar (Fig. 2). The identity of Y also affects the degree of bond breaking in the transition state structures for cleavage. For example, C–C cleavage is well advanced in **5D**$^{\bullet+\ddagger}$ but has barely begun in **7D**$^{\bullet+\ddagger}$ (Fig. 2).

Why are the barriers for oximes and silyl oximes lower than those for aldehydes and ketones? From the energies shown in Table 3, it appears that having X = NOR rather than X=O pulls down the energies of **B**$^{\bullet+\ddagger}$, **C**$^{\bullet+}$ and **D**$^{\bullet+\ddagger}$ relative to that of **A**$^{\bullet+}$. This is likely due to a combination of effects, whose magnitudes are difficult to assess: differences in O–H and N–H bond strengths (note that N–H bonds tend to be slightly shorter than do the corresponding O–H bonds in intermediates **C**$^{\bullet+}$), [78] differences in the ability of OH and HONH groups to stabilize adjacent carbocations and changes in interactions across the O–N bond upon hydrogen transfer to oximes and silyl oxime ethers. From the energies shown in Table 3, it also appears that having Y=O promotes the cleavage process. This is likely due in large part to the greater strength of C=O bonds than C=C bonds, but it may also be due in part to increased $\sigma_{C-R}\leftrightarrow\sigma^*_{C-Y}$ interactions, which should help to break the C–Y bond, when Y=O. [79]

In the 70 eV electron ionization mass spectra of silyl oxime ethers **11** and **12**, a variety of interesting fragmentation pathways were observed, and the proposed mechanisms are depicted in Scheme 3.

The *tert*-butyl radical (*t*-Bu•) is lost from both isomers of the odd-electron silyl aldoxime and ketoxime species to form corresponding silenium ions (Scheme 3, *m/z* 174, 188). The (*Z*)-silenium ions **A** and (*E*)-silenium ions **B** are observed in the spectra of the respective (*Z*)- and (*E*)-aldoximes as well as ketoximes. Silenium ions **A** are stabilized by the proximal ether functionality, and these intermediates give rise to the iminium dioxosilacycles **C** (*m/z* 132, 146) on loss of the propyl chain either by elimination of propene, as shown, or possibly by loss of the propyl cation. Formation of **C** through an ion-neutral complex instead of the 1,2-elimination is also a possibility that cannot be ruled out [80], but we have not investigated this option theoretically in more detail. Finally, it is also possible that **C** could arise via cyclization of the ionized ether linkage [M^{+}_{ether}] (Scheme 3). The observed formation of the α-ether cleavage fragment **D** (*m/z* 73) supports reaction along this path. Whereas silenium ions **B** are not structurally predisposed to undergo a similar cyclization path, their precursors, the odd electron (*E*)-isomers (R=H, R=CH_3), can form silacycles **C** by isomerization to the (*Z*)-isomers prior to loss of *t*-Bu•. The isomerization of ionized oximes is known

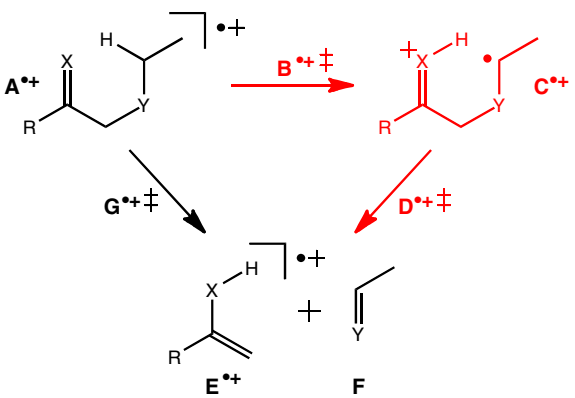

Scheme 2. Nomenclature for the various mechanistic intermediates in Table 3.

Copyright © 2012 John Wiley & Sons, Ltd.

Table 3. Relative free energies [UB3LYP/6-31 G(d); 298.15 K; kcal/mol; normal text] and electronic energies (in parentheses) for species involved in the fragmentation

Class	Compound	R	X	Y	$A^{\bullet+}$	$B^{\bullet+\ddagger}$	$C^{\bullet+}$	$D^{\bullet+\ddagger}$	$\Delta G^{\ddagger}(\Delta E^{\ddagger})$	RDS
Aldehyde/Ketone	**1**	H	O	CH_2	0.0 (0.0)	0.3 (1.5)	1.4 (0.8)	8.6[a] (7.2)	8.6 (7.2)	C–C bond breaking
	2	CH_3	O	CH_2	0.0 (0.0)	−0.2 (1.2)	−0.3 (−0.8)	14.1[a] (12.3)	14.1 (12.3)	C–C bond breaking
	3	H	O	O	0.0 (0.0)				10.9 (11.3)	Concerted
	4	CH_3	O	O	0.0 (0.0)	8.1 (9.5)	9.1 (9.3)	10.6 (10.8)	10.6 (10.8)	C–C bond breaking
Oxime	**5**	H	NOH	CH_2	0.0 (0.0)	−0.5 (0.7)	−6.0 (−6.6)	1.4 (3.4)	1.4 (3.4)	C–C bond breaking
	6	CH_3	NOH	CH_2	0.0 (0.0)	0.3 (1.8)	−6.1 (−6.4)	5.3 (7.3)	5.3 (7.3)	C–C bond breaking
	7	H	NOH	O	0.0 (0.0)	0.0 (1.6)	3.4 (−3.8)	1.6 (−1.2)	0.0 (1.6)	H-transfer
	8	CH_3	NOH	O	0.0 (0.0)	0.2 (1.9)	−4.7 (−5.1)	−0.9 (−1.1)	0.2 (1.9)	H-transfer
Silyl oxime	**9**	H	$NOSiH_3$	CH_2	0.0 (0.0)	1.7 (3.2)	−4.1 (−4.5)	5.1 (7.2)	5.1 (7.2)	C–C bond breaking
					0.0 (0.0)	**0.4 (1.7)**	**−7.2 (−7.4)**	**0.2 (2.4)**	**0.4 (1.7)**	**C–C bond breaking**
	10	CH_3	$NOSiH_3$	CH_2	0.0 (0.0)	2.1 (3.8)	−4.9 (−4.7)	8.1 (10.3)	8.1 (10.3)	C–C bond breaking
					0.0 (0.0)	**1.0 (2.3)**	**−8.1 (−7.9)**	**3.6 (5.4)**	**3.6 (5.4)**	**C–C bond breaking**
	11	H	$NOSiH_3$	O	0.0 (0.0)	0.9 (2.4)	−3.6 (−4.2)	−1.4 (−1.4)	0.9 (2.4)	H-transfer
					0.0 (0.0)	**−0.7 (0.5)**	**−7.1 (−7.6)**	**−4.5 (−4.8)**	**−0.7 (0.5)**	**H-transfer**
	12	CH_3	$NOSiH_3$	O	0.0 (0.0)	0.9 (2.4)	−5.1 (−5.3)	− 0.5 (−1.1)	0.9 (2.4)	H-transfer
					0.0 (0.0)	**−0.6 (0.6)**	**−10.7 (−10.3)**	**−4.1 (−5.0)**	**−0.6 (0.6)**	**H-transfer**

[a]Single-point energies with UB3LYP/6-31 G(d) on geometries optimized with UMP2/6-31G(d); for these structures, convergence problems were encountered when using UB3LYP/6-31G(d). Bold numbers are relative energies calculated using UB3LYP/6-311++G(2d,2p).

Copyright © 2012 John Wiley & Sons, Ltd.

from condensed phase acidic solutions. [81] It has to be stated that this might not be applicable in the gas phase and that $[M + H]^+$ oximes might behave differently than $M^{+\bullet}$ oximes. However, gas-phase ^{1}H NMR studies on rotational barriers of neutral amides [82] and *N*,*N*-dialkylformamide [83] showed that barrier heights of ~20 kcal/mol do not preclude isomerization, and so it seems reasonable to assume that the (*E*)-to-(*Z*) isomerization barrier height in the ionized state of 16.2 kcal/mol is not prohibitive in the gas phase. The odd-electron (*E*)-isomers are structurally poised for γ-hydrogen atom abstraction. Subsequent loss of propanal via α,β-bond scission occurs to give the McLafferty rearrangement fragments. The facile loss of *t*-Bu• occurs here as well to yield **E**, which likely forms the isomeric 5-membered silacycles (*m/z* 116, 130) as depicted, whereas a three-membered silacycle was excluded as a realistic option. The McLafferty rearrangement with loss of *t*-Bu• is observed for both aldoxime isomers and both ketoxime isomers, although the propensity for cleavage via the McLafferty rearrangement is higher for the (*E*)-isomers.

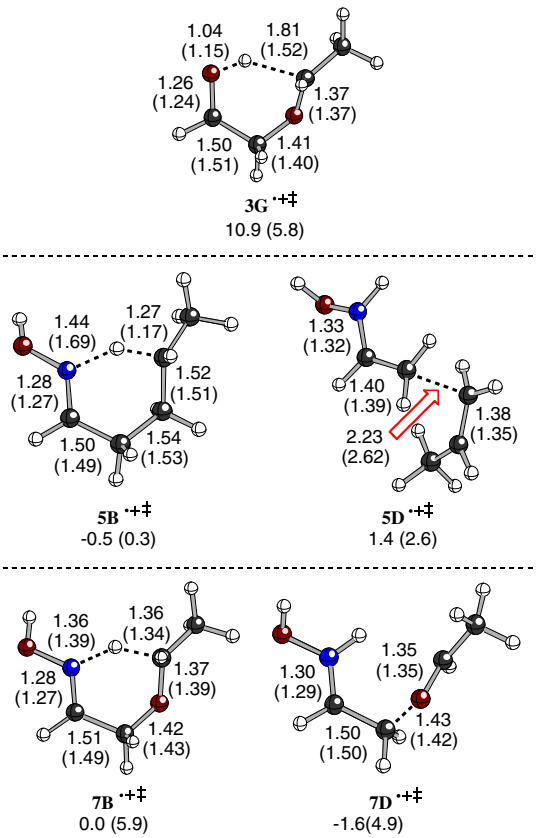

Figure 2. Computed geometries and free energies (298.15 K; kcal/mol; relative to $\mathbf{A}^{\bullet+}$ for each system) for representative transition state structures. Distances (Å) and energies computed with UB3LYP/6-31G(d) are in normal type, whereas those computed with UM06-2X/6-31G(d) are in parentheses.

As reported previously, [84] a characteristic fragmentation observed in the mass spectra of silyl ketoxime ethers is the N–O bond cleavage (Scheme 4). The observed fragment ion is presumably a nitrilium ion derived via a 1,2-shift [85] of the alkyl side-chain concomitant with loss of the silyloxy radical. Nitrilium ions commonly are derived from iminium species. [86] Whereas both isomers of silyl ketoxime ether **10** undergo major N–O bond cleavage, this mode of fragmentation is not significant for any of the ketoximes (Fig. 3). Furthermore, the (*Z*)- and (*E*)-isomers of silyl ketoxime ether **12** appear to undergo N–O cleavage to only a small extent, possibly because the migratory aptitude of the oxygen-containing side-chain is diminished. [85] However, the scarcity of the nitrilium ions for these isomers may be due to the facile loss of acetonitrile, giving the more stable oxonium ion species (*m/z* 73). The *m/z* 73 fragment is also populated by the paths described earlier (e.g. species **D** in Scheme 3). Along these lines, the *m/z* 73 fragment derived from oxime **8** is the result of the McLafferty rearrangement, which was shown to be the predominant fragmentation for all oximes. The N–O cleavage mode is negligible for all aldoximes and silyl aldoximes (Scheme 4, where R=H). Figure 3 clearly shows the impact of oxygen substitution adjacent to the radical-forming center during McLafferty rearrangement.

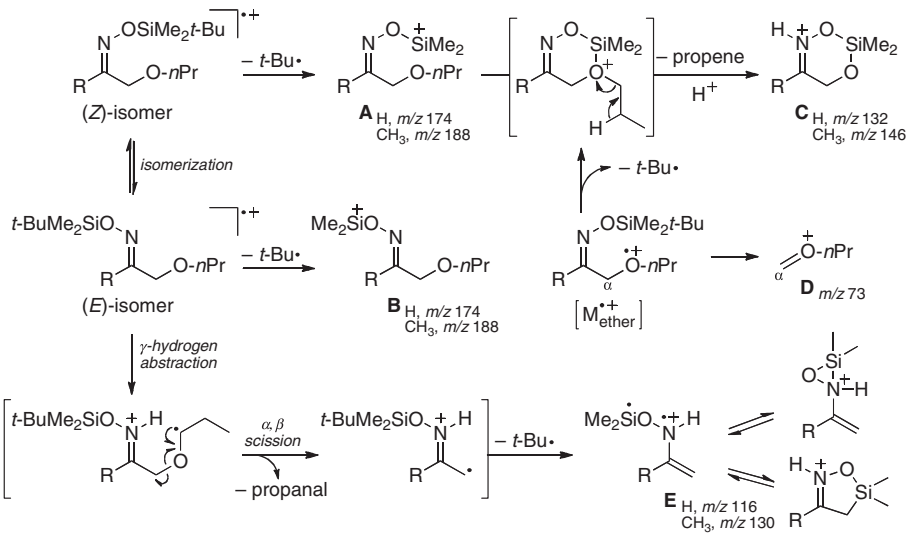

Scheme 3. The proposed fragmentation mechanisms for silyl oxime ethers **11** and **12**.

Copyright © 2012 John Wiley & Sons, Ltd.

Journal of MASS SPECTROMETRY

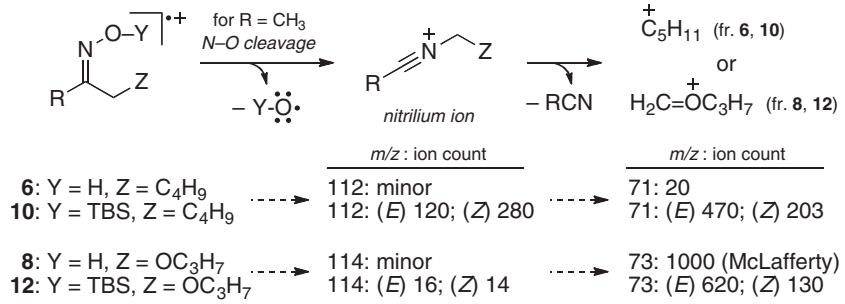

Scheme 4. The proposed fragmentation mechanism for the N–O bond cleavage followed by loss of RCN from the silyl ketoximes **10** and **12**.

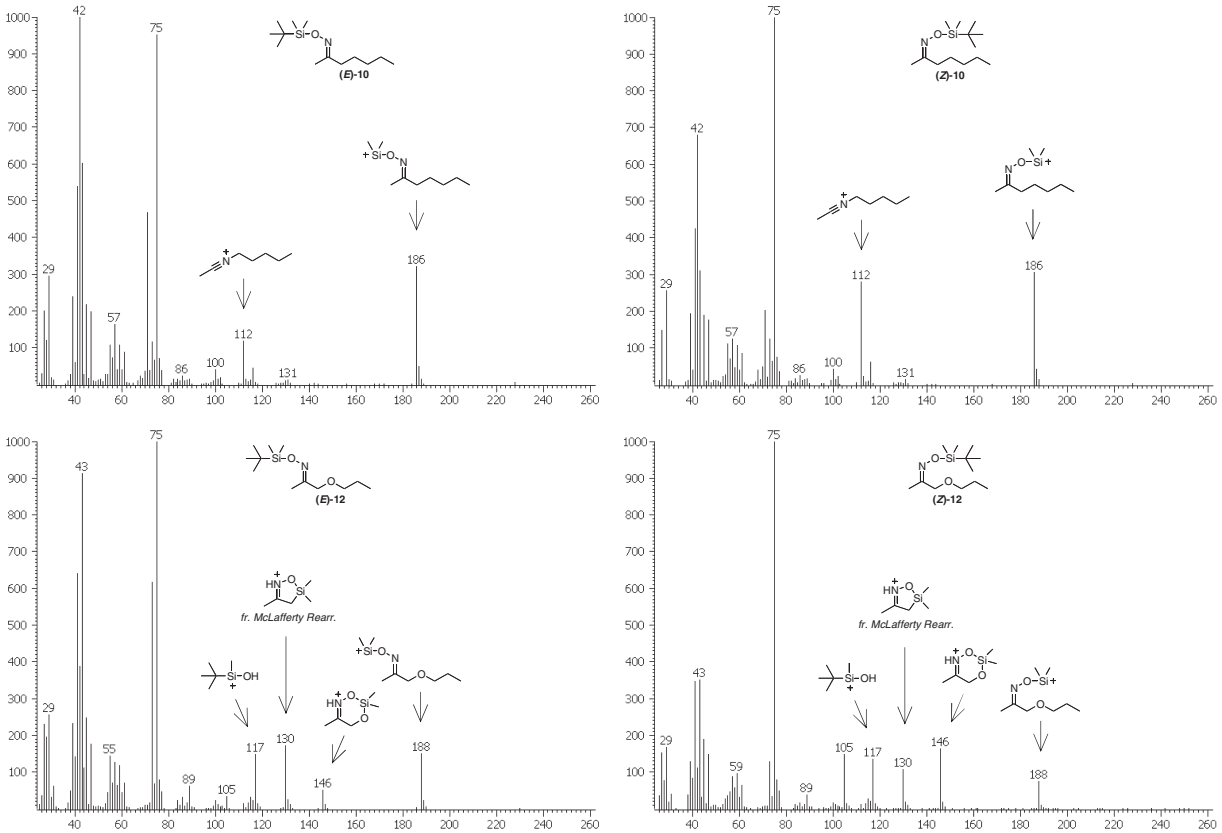

Figure 3. The influence of β-CH_2 *versus* β-O on the fragmentation of silyl oxime ethers. The ketoxime isomers (top pair) do not exhibit significant α,β-bond scission (McLafferty rearrangement), unlike the oxygen-substituted isomers (bottom pair).

CONCLUSIONS AND FUTURE DIRECTIONS

We have shown experimentally and theoretically that a set of 12 synthesized model compounds, comprised of carbonyl, oxime and silyl oxime ether molecules, undergo the McLafferty rearrangement upon 70 eV electron ionization to varying extents, with the silyl oximes that lack γ-radical stabilization (e.g. β-oxygen substitution) having the lowest incidence of such rearrangement. The McLafferty rearrangement is enhanced, relative to other primary fragmentation processes, by oximes (*vs* carbonyl), oxygen at the β-position (*vs* β-methylene) and ketones (*vs* aldehydes). The McLafferty reverse charge rearrangement was also observed to varying extent for most molecules investigated, and its contribution should be added to the relative contribution of the McLafferty rearrangement to compare the overall contribution compared with the other primary fragmentation reactions. The results of density functional calculations indicated that most compounds undergo a stepwise McLafferty rearrangement and that both C–C bond breaking and H-transfer could be the rate-determining step. Only $HC(O)CH_2OC_3H_7$ was predicted to undergo fragmentation via a concerted mechanism. For the silyl oxime ethers, the McLafferty rearrangement was accompanied by the subsequent loss of the *t*-butyl radical. Finally, we observed that oximes and silyl oxime ethers were obtained as both the (*E*)- and (*Z*)-isomers and that the extent of the McLafferty rearrangement was higher in the (*E*)-isomers. Future work will include the synthesis of some novel oximes and additional calculations to help elucidate the mechanisms of the unusual fragmentation reactions we have observed in this work and to study the McLafferty reverse charge rearrangement of oximes in more detail.

 Copyright © 2012 John Wiley & Sons, Ltd.

Acknowledgements

We thank Ms Aiqin Fang for early contributions and Ms Xue Shi for assistance with mass spectra acquisition. The authors also thank Dr Nico M. M. Nibering (Free University Amsterdam) for his insightful comments. This work was supported by NIH grant 1RO1GM087735-3 (X.Z.) and NSF grant CHE-030089 (with the Pittsburgh Supercomputer Center, O.G, J.G.H, D.J.T.).

Supporting Information

Supporting information may be found in the online version of this article.

REFERENCES

[1] P. J. O'Brien, A. G. Siraki, N. Shangari. Aldehyde sources, metabolism, molecular toxicity mechanisms, and possible effects on human health. *Crit. Rev. Toxicol.* **2005**, *35*, 609.
[2] M. K. Campbell, S. O. Farrell. Biochemistry (5th edn). Cengage Learning: Independence, KY, **2006**, 579, ISBN 0534405215.
[3] L. Laffel. Ketone bodies: a review of physiology, pathophysiology and application of monitoring to diabetes. *Diabetes Metab. Res. Rev.* **1999**, *15*(6), 412.
[4] A. Zajdel, A. Wilczok, J. Slowinski, J. Orchel, U. Mazurek. Aldehydic lipid peroxidation products in human brain astrocytomas. *J. Neurooncol* **2007**, *84*(2), 167.
[5] A. E. Kitabchi, G. E. Umpierrez, M. B. Murphy, R. A. Kreisberg. Hyperglycemic crises in adult patients with diabetes. *Diabetis Care*, **2006**, *29*(12), 2739.
[6] S. Rochfort. Metabolomics reviewed: a new "omics" platform technology for systems biology and implications for natural products research. *J. Nat. Prod.* **2005**, *68*(12), 1813.
[7] E. A. Mazzio, B. Smith, K. F. A. Soliman. Evaluation of endogenous acidic metabolic products associated with carbohydrate metabolism in tumor cells. *Cell Biol. Toxicol.* **2010**, *26*(3), 177.
[8] M. G. Barderas, C. M. Laborde, M. Posada, F. de la Cuesta, I. Zubiri, F. Vivanco, G. Alvarez-Llamas. Metabolomic profiling for identification of novel potential biomarkers in cardiovascular diseases. *J. Biomed. Biotech.*, *2011*, Article ID 790132, 9 DOI:10.1155/2011/790132
[9] J. Iglesias, J. M. Gallardo, I. Medina. Determination of carbonyl compounds in fish species samples with solid-phase microextraction with on-fibre derivatization. *Food Chem.* **2010**, *123*(3), 771.
[10] S. J. Mattingly, T. Xu, M. H. Nantz, R. M. Higashi, T. W.-M. Fan. A carbonyl capture approach for profiling oxidized metabolites in cell extracts. *Metabolomics* **2012**, accepted (DOI: 10.1007/s11306-011-0395-z).
[11] N. Andrási, A. Helenkár, G. Záray, A. Vasanits, I. Molnár-Perl. Derivatization and fragmentation pattern analysis of natural and synthetic steroids, as their trimethylsilyl (oxime) ether derivatives by gas chromatography mass spectrometry: Analysis of dissolved steroids in wastewater samples. *J. Chromatogr. A* **2011**, *1218*(14), 1878.
[12] M. Brokl, A. C. Soriab, I. Martínez-Castroa, M. L. Sanza, A. I. Ruiz-Matute. Characterization of O-trimethylsilyl oximes of trisaccharides by gas chromatography–mass spectrometry. *J. Chromatogr. A* **2009**, *1216*(22), 4689.
[13] Z. Fűzfai, I. Boldizśar, I. Molńar-Perl. Characteristic fragmentation patterns of the trimethylsilyl and trimethylsilyl –oxime derivatives of various saccharides as obtained by gas chromatography coupled to ion-trap mass spectrometry. *J. Chromatogr. A* **2008**, *1177*(1), 183.
[14] K. Horváth, I. Molńar-Perl. Simultaneous quantitation of mono-, di- and trisaccharides as their TMS ether oxime derivatives by GC-MS: I. In model solutions. *Chromatographia* **1997**, *45*(1), 321.
[15] I. Molńar-Perl, K. Horváth. Simultaneous quantitation of mono-, di- and trisaccharides as their TMS ether oxime derivatives by GC-MS: I. In honey. *Chromatographia* **1997**, *45*(1), 328.
[16] Á. Sebőka, K. Sezerc, A. Vasanits-Zsigrai, A. Helenkára, G. Záraya, I. Molnár-Per. Gas chromatography–mass spectrometry of the trimethylsilyl (oxime) ether/ester derivatives of cholic acids: Their presence in the aquatic environment. *J. Chromatogr. A* **2008**, *1211*(1–2), 104.
[17] Z. F. Katona, P. Sass, I. Molnár-Perl. Simultaneous determination of sugars, sugar alcohols, acids and amino acids in apricots by gas chromatography–mass spectrometry. *J. Chromatogr. A* **1999**, *847*(1–2), 91.
[18] N. Nazarpack-Kandlousy, M. I. Nelen, V. Goral, A. V. Eliseev. Synthesis and mass spectrometry studies of branched oxime ether libraries. Mapping the substitution motif via linker stability and fragmentation pattern. *J. Org. Chem.* **2002**, *67*(1), 59.
[19] A. J. C. Nicholson. Photochemical decomposition of the aliphatic methyl ketones. *Trans. Faraday Soc.* **1954**, *50*, 1067.
[20] F. W. McLafferty. Mass spectrometric analysis. Broad applicability to chemical research. *Anal. Chem.* **1956**, *28*(2), 306.
[21] V. Ramesh, R. Srinivas, G. Kumaraswamy, B. Markondaiah. Diastereoselectivity in the McLafferty-type rearrangement of protonated precursors of belactosin derivatives using electrospray ionization (ESI) and atmospheric pressure photo ionization (APPI) tandem mass spectrometry. *J. Mass Spectrom.* **2009**, *44*(2), 285.
[22] S.-Z. Yang, X.-Y. Liu, B.-Z. Mu. The McLafferty rearrangement in the Glu residue in a cyclic lipopeptide determined by Q-TOF MS/MS. *J. Mass Spectrom.* **2008**, *43*(12), 1673.
[23] D. Norberg, N. Salhi-Benachenhou. McLafferty rearrangement of the radical cations of butanal and 3-fluorobutanal: A theoretical investigation of the concerted and stepwise mechanisms. *J. Comput. Chem.* **2008**, *29*(3), 392.
[24] M. J. Van Stipdonk, D. R. Kerstetter, C. M. Leavitt, G. S. Groenewold, J. Steill, J. Oomens. Spectroscopic investigation of H atom transfer in a gas-phase dissociation reaction: McLafferty rearrangement of model gas-phase peptide ions. *Phys. Chem. Chem. Phys.* **2008**, *10*(22), 3209.
[25] J. S. Grossert, M. C. Cook, R. L. White. The influence of structural features on facile McLafferty-type, even-electron rearrangements in tandem mass spectra of carboxylate anions. *Rapid Commun. Mass Spectrom.* **2006**, *20*(10), 1511.
[26] L. V. Klyba, N. A. Nedolya, N. I. Shlyakhtina, E. R. Zhanchipova. Mass spectra of new functionally substituted heterocycles: V. First example of McLafferty rearrangement in the series of 5-(1-ethoxyethoxy)-2, 3-dihydro-pyridines and 3-(1-ethoxyethoxy)pyridines derived from alpha-lithiated 1-(1-ethoxyethoxy)-allene and methoxymethyl isothiocyanate. *Rus. J. Org. Chem.* **2005**, *41*(10), 1544.
[27] J. Loos, D. Schröder, H. Schwarz. Diastereoselectivity in the McLafferty rearrangement of photoionized 3-methyl valeramide. *J. Org. Chem.* **2005**, *70*(3), 1073.
[28] J. Loos, D. Schröder, H. Schwarz, R. Thissen, O. Dutuit. Competitive reactions and diastereoselective C-H bond activation in the McLafferty rearrangement of photoionized 3-methyl valeramide. *Int. J. Mass Spectrom.* **2005**, *240*(2), 121.
[29] F. Tureček. McLafferty and related rearrangements Encyclopedia of Mass Spectrometry, Volume 4, Fundamentals of and applications to organic (and organometallic) compounds, N. M. M. Nibbering (Ed). Elsevier: Amsterdam, **2005**. ; Chapter 4, 396
[30] G. A. Olah, T. Mathew, A. Goeppert, G. Rasul, G. K. S. Prakash, P. M. Esteves. Carbocationic rearrangement cation and protonated of pivaloyl pivalaldehyde in superacid medium: A novel solution equivalent of the McLafferty rearrangement. *J. Am. Soc. Mass Spectrom.* **2004**, *15*(7), 959.
[31] G. van der Rest, L. B. Jensen, S. A. Azeim, P. Mourgues, H. E. Audier. Reactions of [NH_3^+, H_2O] with carbonyl compounds: A McLafferty rearrangement within a complex? *J. Am. Soc. Mass Spectrom.* **2004**, *15*(7), 966.
[32] V. Anbalagan, J. N. Patel, G. Niyakorn, M. J. Van Stipdonk. McLafferty-type rearrangement in the collision-induced dissociation of Li^+, Na^+ and Ag^+ cationized esters of N-acetylated peptides. *Rapid Commun. Mass Spectrom.* **2003**, *17*(4), 291.
[33] S. T. Oh, J. C. Choe, M. S. Kim. Photodissociation dynamics of n-butylbenzene molecular ion. *J. Phys. Chem.* **1996**, *100*(32), 13367.
[34] M. Takayama. Metastable McLafferty rearrangement reaction in the electron-impact ionization of stearic-acid methyl-ester. *Int. J. Mass Spectrom. Ion Proc.* **1995**, *144*(3), 199.
[35] S. Dohmeierfischer, N. Kramer, H. F. Grutzmacher. Rearrangement by intermediate ion/neutral complexes during the McLafferty fragmentation of unsaturated-ketones. *Eur. Mass Spectrom.* **1995**, *1*(1), 3.
[36] D. V. Kenny, S. V. Olesik. APCI low-energy collision-induced dissociation fragmentation of protonated ortho silicates – McLafferty or ion-neutral complex rearrangement. *J. Am. Soc. Mass Spectrom.* **1994**, *5*(6), 544.
[37] R. D. Bowen, A. Maccoll. Low-energy, low-temperature mass spectra 16. The predominance of peaks arising from single and double McLafferty rearrangements in the mass spectra of ketoximes. *Int. J. Mass Spectrom. Ion. Proc.* **1992**, *122*, 337.
[38] P. P. Trigueros, J. Casanovas, C. Aleman, M. C. Vega. A MNDO and AM1 quantum chemical study of the reaction mechanism of the

Copyright © 2012 John Wiley & Sons, Ltd.

McLafferty type rearrangement in the butanal radical cation. *Theochem - J. Mol. Struct.* **1992**, *277*, 117.
[39] M. B. Stringer, D. J. Underwood, J. H. Bowie, C. E. Allison, K. F. Donchi, P. J. Derrick. Is the McLafferty rearrangement of ketones concerted or stepwise – the application of kinetic isotope effects. *Org. Mass Spectrom.* **1992**, *27*(3), 270.
[40] R. F. Liu, P. Pulay. Ab Initio evidence for the stepwise mechanism of the McLafferty rearrangement of the butanal radical cation. *J. Comput. Chem.* **1992**, *13*(2), 183.
[41] H. Budzikiewics, P. Bold. Mass spectroscopic fragmentation reactions 33. A McLafferty rearrangement in an even-electron system – C_3H_6 elimination from the alpha-cleavage product of tri-normal-butylamine. *Org. Mass Spectrom.* **1991**, *26*(8), 709.
[42] T. H. Osterheld, J. I. Brauman. Infrared multiple photon dissociation of butyrophenone cation – a stepwise McLafferty reaarangement. *J. Am. Chem. Soc.* **1990**, *112*(5), 2014.
[43] Q. M. Zha, R. N. Hayes, T. Nishimura, G. G. Meisels, M. L. Gross. A study of the metastable dissociations of formate esters – a McLafferty rearrangement to a distonic radical cation. *J. Phys. Chem.* **1990**, *94*(4), 1286.
[44] F. Tureček, D. E. Drinkwater, F. W. McLafferty. The stepwise nature of the γ-hydrogen rearrangement in unsaturated ions. *J. Am. Chem. Soc.* **1990**, *112*(3), 993.
[45] G. Bouchoux, Y. Hoppilliard, J. Tortajada. Structure et role des complexes ions/molecules durant le rearrangement de McLafferty: Etude ab initio du systeme $[CH_2{=}CHOH]^{+\bullet}/CH_2{=}CH_2$. *Int. J. Mass Spectrom. Ion Proc.* **1989**, *90*(3), 197.
[46] D. M. Bernard, A. J. Stace. Intramolecular ion/molecule reactions in clusters. Evidence of multiple McLafferty rearrangements in protonated *n*-butanoic acid clusters. *Int. J. Mass Spectrom Ion Proc.* **1988**, *84*(1–2), 215.
[47] B. L. M. Van Baar, J. K. Terlouw, S. Akkök, W. Zummack, H. Schwarz. On the structure of the $C_2H_4O_2$ neutrals (acetic acid versus 1, 1-dihydroxyethene) generated from ionized *n*-hexanoic acid and *n*-butyl acetate in the gas phase. Implications for the mechanism of the McLafferty rearrangement. *Int. J. Mass Spectrom Ion Proc.* **1987**, *81*, 217.
[48] T.-K. Ha, C. Radloff, M. T. Nguyen. An ab initio study on the McLafferty-type rearrangement in the butanal radical cation ($CHOCH_2CH_2CH_3^{+\bullet}$). *J. Phys. Chem.* **1986**, *90*(13), 2991.
[49] M. Zollinger, J. Seibl. Comparative investigation of reactivities in even- and odd-electronic cations: McLafferty rearrangements. *Int. J. Mass Spectrom Ion Phys.* **1983**, *47*, 363.
[50] F. Tureček, V. Hanuš. Charge distribution between formally identical fragments: the McLafferty rearrangement. *Org. Mass Spectrom.* **1980**, *15*(1), 8.
[51] J. F. Litton, T. L. Kruger, R. G. Cooks. Alkane elimination in mass spectrometry. A counterpart to the McLafferty rearrangement. *J. Am. Chem. Soc.* **1976**, *98*(7), 2011.
[52] K. Levsen, H. Schwarz. Structure of gaseous $C_2H_4O_2^{+\bullet}$ ions formed by McLafferty rearrangement from aliphatic acids. *J. Chem Soc. Perkin Trans. 2*, **1976**, *11*, 1231.
[53] A. J. Breijer, H. M. A. Buurmans, B. Van De Graaf, P. J. W. Schuijl, A. P. G. Kieboom. Electron-impact induced fragmentation of labeled 3-(m-nitrobenzoyl)-2-methylpropanoic acids. Evidence for a stepwise McLafferty rearrangement. *Tetrahedron* **1974**, *30*(16), 2797.
[54] D. G. I. Kingston, J. T. Bursey, M. M. Bursey. Intramolecular hydrogen transfer in mass spectra. II. The McLafferty rearrangement and related reactions. *Chem. Rev.* **1974**, *74*(2), 215.
[55] G. Eadon. Mechanism of the double McLafferty rearrangement. *J. Am. Chem. Soc.* **1972**, *94*(25), 8938.
[56] J. Diekman, J. K. MacLeod, C. Djerassi, J. D. Baldeschwieler. Determination of the structures of the ions produced in the single and double McLafferty rearrangements by ion cyclotron resonance spectroscopy. *J. Am. Chem. Soc.* **1969**, *91*(8), 2069.
[57] F. P. Boer, T. W. Shannon, F. W. McLafferty. The electronic structure of the six-membered cyclic transition state in some γ-hydrogen rearrangements. *J. Am. Chem. Soc.* **1968**, *90*(26), 7239.
[58] K. J. Jobst, R. D. Bowen, J. K. Terlouw. The dissociation chemistry of low-energy N-formylethanolamine ions: Hydrogen-bridged radical cations as key intermediates. *Int. J. Mass Spectrom.* **2011**, *306*(1), 9.
[59] S. M. Schildcrout, J. Masnovi. Gaseous cation chemistry and chain-length effects in electron ionization and collision-induced dissociation mass spectra of symmetric 1,n-bis(9-anthracenyl) alkanes. *J. Mass Spectrom.* **2010**, *46*(6), 572.
[60] Y. A. Jeilani, B. H. Cardelino, V. M. Ibeanusi. Positive chemical ionization triple-quadrupole mass spectrometry and ab initio computational studies of the multi-pathway fragmentation of phthalates. *J. Mass Spectrom.* **2010**, *45*(6), 678.
[61] G. Bouchoux, Y. Hoppilliard, P. Longevialle. The role of ion-neutral complexes in the fragmentation of hexanal radical cations. *Rapid Commun. Mass Spectrom.* **1987**, *1*(6) 94–96
[62] O. K. Rice, H. C. Ramsperger. Theories of unimolecular gas reactions at low pressures. *J. Am. Chem. Soc.* **1927**, *49*(7), 1617.
[63] http://iupac.org/publications/pac/pdf/1996/pdf/6801x0149.pdf
[64] http://goldbook.iupac.org/R05391.html
[65] C. E. Hudson, L. L. Griffin, D. J. McAdoo. Ab initio and RRKM evidence that the McLafferty rearrangement of ionized *n*-butanal is stepwise. *Org. Mass Spectrom.* **1989**, *24*(10), 866.
[66] (a) A. D. Becke. Density-functional thermochemistry. III. The role of exact exchange. *J. Chem. Phys.* **1993**, *98*(7), 5648. (b) A. D. Becke. A new mixing of Hartree-Fock and local density-functional theories. *J. Chem. Phys.* **1993**, *98*(2), 1372. (c) C. Lee, W. Yang, R. G. Parr. Development of the Colle-Salvetti correlation-energy formula into a functional of the electron density. *Phys. Rev. B.* **1988**, *37*(2), 785. (d) P. J. Stephens, F. J. Devlin, C. F. Chabalowski, M. J. Frisch. Ab initio calculation of vibrational absorption and circular dichroism spectra using density functional force fields. *J. Phys. Chem.* **1994**, *98*(45), 11623.
[67] M. J. Frisch, G. W. Trucks, H. B. Schlegel, G. E. Scuseria, M. A. Robb, J. R. Cheeseman, J. A., Montgomery, Jr. T. Vreven, K. N. Kudin, J. C. Burant, J. M. Millam, S. S. Iyengar, J. Tomasi, V. Barone, B. Mennucci, M. Cossi, G. Scalmani, N. Rega, G. A. Petersson, H. Nakatsuji, M. Hada, M. Ehara, K. Toyota, R. Fukuda, J. Hasegawa, M. Ishida, T. Nakajima, Y. Honda, O. Kitao, H. Nakai, M. Klene, X. Li, J. E. Knox, H. P. Hratchian, J. B. Cross, V. Bakken, C. Adamo, J. Jaramillo, R. Gomperts, R. E. Stratmann, O. Yazyev, A. J. Austin, R. Cammi, C. Pomelli, J. W. Ochterski, P. Y. Ayala, K. Morokuma, G. A. Voth, P. Salvador, J. J. Dannenberg, V. G. Zakrzewski, S. Dapprich, A. D. Daniels, M. C. Strain, O. Farkas, D. K. Malick, A. D. Rabuck, K. Raghavachari,J. B. Foresman, J. V. Ortiz, Q. Cui, A. G. Baboul, S. Clifford, J. Cioslowski, B. B. Stefanov, G. Liu, A. Liashenko, P. Piskorz, I. Komaromi, R. L. Martin, D. J. Fox, T. Keith, M. A. Al-Laham, C. Y. Peng, A. Nanayakkara, M. Challacombe, P. M. W. Gill, B. Johnson, W. Chen, M. W. Wong, C. Gonzalez, J. A. Pople. GAUSSIAN03, Revision D.01, Gaussian, Inc., Wallingford CT, **2004**.
[68] For leading references, see: (a) O. Wiest, D. C. Montiel, K. N. Houk. Quantum mechanical methods and the interpretation and prediction of pericyclic reaction mechanisms. *J. Phys. Chem. A* **1997**, *101*(45), 8378. (b) V. A. Guner, K. S. Khuong, K. N. Houk, A. Chuma, P. Pulay. The performance of the Handy/Cohen functionals, OLYP and O3LYP, for the computation of hydrocarbon pericyclic reaction activation barriers. *J. Phys. Chem.* **2004**, *108*, 2959. (c) N. Saettel, J. Oxgaard, O. Wiest. Pericyclic reactions of radical cations. *Eur. J. Org. Chem.* **2001**, *8*, 1429. (d) O. Wiest, J. Oxgaard, N. J. Saettel. Structure and reactivity of hydrocarbon radical cations. *Adv. Phys. Org. Chem.* **2003**, *38*, 87.
[69] Y. Zhao, D. G. Truhlar. The M06 suite of density functionals for main group thermochemistry, thermochemical kinetics, noncovalent interactions, excited states, and transition elements: two new functionals and systematic testing of four M06-class functionals and 12 other functionals. *Theor. Chem. Acc.* **2008**, *120*(1–3), 215.
[70] C. Møller, M. S. Plesset. Note on an approximation treatment for many-electron systems. *Phys. Rev.* **1934**, *46*, 618.
[71] M. Gerenkamp, S. Grimme. Spin-component scaled second-order Møller–Plesset perturbation theory for the calculation of molecular geometries and harmonic vibrational frequencies. *Chem. Phys. Lett.* **2004**, *392*(1–3), 229.
[72] M. J. Frisch, G. W. Trucks, H. B. Schlegel, G. E. Scuseria, M. A. Robb, J. R. Cheeseman, G. Scalmani, V. Barone, B. Mennucci, G. A. Petersson, H. Nakatsuji, M. Caricato, X. Li, H. P. Hratchian, A. F. Izmaylov, J. Bloino, G. Zheng, J. L. Sonnenberg, M. Hada, M. Ehara, K. Toyota, R. Fukuda, J. Hasegawa, M. Ishida, T. Nakajima, Y. Honda, O. Kitao, H. Nakai, T. Vreven, J. A. Montgomery, Jr., J. E. Peralta, F. Ogliaro, M. Bearpark, J. J. Heyd, E. Brothers, K. N. Kudin, V. N. Staroverov, T. Keith, R. Kobayashi, J. Normand, K. Raghavachari, A. Rendell, J. C. Burant, S. S. Iyengar, J. Tomasi, M. Cossi, N. Rega, J. M. Millam, M. Klene, J. E. Knox, J. B. Cross, V. Bakken, C. Adamo, J. Jaramillo, R. Gomperts, R. E. Stratmann, O. Yazyev, A. J. Austin, R. Cammi, C. Pomelli, J. W. Ochterski, R. L. Martin, K. Morokuma, V. G. Zakrzewski, G. A. Voth, P. Salvador, J. J. Dannenberg, S. Dapprich, A. D. Daniels, O. Farkas, J. B. Foresman, J. V. Ortiz, J. Cioslowski, D. J. Fox, GAUSSIAN09, Revision B.01, Gaussian, Inc.: Wallingford CT, **2010**.

 Copyright © 2012 John Wiley & Sons, Ltd.

[73] (a) C. Gonzalez, H. B. Schlegel. Reaction path following in mass-weighted internal coordinate. *J. Phys. Chem.* **1990**, *94*(14), 5523. (b) K. Fukui. The path of chemical reactions - the IRC approach. *Acc. Chem. Res.* **1981**, *14*(12), 363.
[74] N. Müller, A. Falk, G. Gsaller. *Ball & Stick V.4.0a12*, molecular graphics application for MacOS computers. Johannes Kepler University: Linz, **2004**.
[75] http://webbook.nist.gov/cgi/cbook.cgi?ID=C66251&Units=SI&Mask=200
[76] http://webbook.nist.gov/cgi/cbook.cgi?ID=C110430&Units=SI&Mask=200
[77] (a) All attempts to find concerted transition state structures for the other systems failed at the UB3LYP/6-31 G(d) level of theory. (b) For comparison, using SCS-UMP2/6-31 G(d) calculations, relative energies for compound 5 are predicted to be: $\mathbf{A}^{\bullet+} = 0.0$, $\mathbf{B}^{\bullet+\ddagger} = -4.7$, $\mathbf{C}^{\bullet+} = -14.0$, $\mathbf{D}^{\bullet+\ddagger} = 5.4$ (all in kcal/mol). (c) UM06-2X/6-31 G(d) was also used and similar reactivity trends were obtained, although, as shown in Figure 2, geometries for hydrogen transfer transition state structures vary slightly.
[78] J. Lind, G. Merenyi. Kinetic and thermodynamic properties of the aminoxyl ($NH_2O^{\bullet}$) radical. *J. Phys. Chem. A* **2006**, *110*(1), 192.
[79] See Supporting Information for information on conformational preferences of radical cation reactants and their neutral counterparts.
[80] (a) T. H. Morton. Collisional Activation and Dissociation: Via Ion-Neutral Complexes Encyclopedia of Mass Spectrometry, Volume 1, Theory and Ion Chemistry, P. B. Armentrout (Ed.) Elsevier: Amsterdam, **2003**, 467 (b) T. H. Morton. Theoretical Models for Ion-Neutral Complexes in Unimolecular Ion Decompositions Encyclopedia of Mass Spectrometry, Volume 4, Fundamentals of and applications to organic (and organometallic) compounds, N. M. M. Nibbering (Ed.) Elsevier: Amsterdam, **2005**, 165.
[81] S. Nsikabaka, W. Harb, M. F. Ruiz-López. The role of water on the acid-promoted E/Z isomerization of oximes in aqueous solution. *J. Mol. Struct. (THEOCHEM)*, **2006**, *764*(1–3), 161.
[82] M. Felgel. Rotation barriers of amides in the gas phase. *J. Phys. Chem.* **1983**, *87*, 3054.
[83] C. B. LeMaster, N. S. True. Gas-phase NMR study of torsional barriers in N,N-diethyl- and N,N-diisopropylformamide. Medium effects on kinetic parameters. *J. Phys. Chem.* **1989**, *93*, 1307.
[84] D. Rusinska-Roszak, M. Lozynski. Gas chromatographic and mass spectrometric studies on trimethylsilyl derivatives of hydroxyoximes. *J. Prakt. Chem.* **1990**, *332*(3), 300.
[85] R. G. Cooks, A. G. Varvoglis. The characteristics of oxime ethers upon electron-impact. *Org. Mass Spectrom.* **1971**, *5*(6), 687.
[86] K. Zaitsu, M. Katagi, H. T. Kamata, A. Miki, H. Tsuchihashi. Discrimination and identification of regioisomeric β-keto analogs of 3,4-methylenedioxyamphetamines by gas chromatography–mass spectrometry. *Forensic Toxicol.* **2008**, *26*(2), 45.

Copyright © 2012 John Wiley & Sons, Ltd.